Comparison of the WRF and MM5 Models for Simulation of Heavy Rainfall along the Baiu Front

Hiroyuki Kusaka[1], Andrew Crook[2], Jimy Dudhia[2], and Koji Wada[1]
[1]*Fluid Dynamics Sector, Central Research Institute of Electric Power Industry, Abiko, Japan*
[2]*Mesoscale and Microscale Meteorology Division, National Center for Atmospheric Research, Boulder, CO, USA*

Abstract

A comparison of WRF and MM5 models was conducted to investigate the differences in the performance for a simulation of a heavy rainfall event along the Baiu front. The simulated precipitation pattern from WRF and MM5 roughly agrees with the observations. However, details are different among WRF, MM5, and observations. The position of the heaviest rainfall is found onshore in WRF and the observations, whereas it is found offshore in MM5. The difference in the position is more clearly found in the vertical velocity field. Additionally, the vertical velocity field of WRF is more detailed than that of MM5. Power spectral density of the vertical velocity clearly shows the difference. Sensitivity experiments indicate that this is due to the differences in the numerical scheme for the model dynamics, not in the cloud microphysics.

1. Introduction

In recent years, natural disasters such as heavy rainfall along the Baiu front occurred frequently, and thus the development of a non-hydrostatic Numerical Weather Prediction (NWP) model has been desired. A new compressible non-hydrostatic NWP model, Weather Research and Forecasting (WRF) model has been developed by the collaboration among the National Center for Atmospheric Research (NCAR), National Center for Environmental Prediction (NCEP), Forecast System Laboratory of the NOAA (NOAA/FSL), and Air Force Weather Agency (AFWA), etc . The Advanced Research core version of this model (Skamarock et al. 2005) is designed as the next generation model after the PSU/NCAR-MM5 (Dudhia 1993), which has been widely used all over the world. One of the big differences between WRF and MM5 is that the dynamical core of WRF uses high-order accurate discretization schemes for time and space: third-order Runge-Kutta scheme for the time integration, and second- to sixth-order schemes for the advection terms . Another difference is that WRF does not yet include explicit numerical diffusion. The other is that the new microphysics scheme is developed and incorporated into WRF. Many current MM5 users will use WRF for simulation of natural disaster in the near future. However the difference in performance and feature for simulation of heavy rainfall along the Baiu front between WRF and MM5 has not been investigated because it is still under development. In this study, we will compare between WRF and MM5 for the simulation of heavy rain event along the Baiu front, and report the difference in the fundamental properties between the two models.

Corresponding author: Hiroyuki Kusaka, Fluid Dynamics Sector, Central Research Institute of Electric Power Industry, Abiko 270-1194, Japan. E-mail: h-kusaka@criepi.denken.or.jp.
©2005, the Meteorological Society of Japan.

2. Design of numerical simulation

The Baiu front extended from the Sea of Japan to the Pacific Ocean, and heavy rainfall that killed 15 people occurred along the front on July 13th 2004 (Fig. 1). At 0900 JST, a convective line was well developed and produced banded heavy rainfall exceeding 100 mm per three-hours (Fig. 2). This is the historical record. Afterwards, the heavy rainfalls gradually dissipated (supplement 1). In this study, we will conduct numerical simulations of the heavy rainfall using WRF and MM5. We used two nested domains for all simulations. The first (outer) domain is 3600 km by 3360 km in the horizontal direction, which includes Japan, Taiwan, and southern part of Sakhalin (Fig. 3). The second (inner) domain is 1320 km by 1200 km in the horizontal direction. Horizontal grid spacing is set to be 12km and 4km for domains 1 and 2, respectively. The model top is set to be 50 hPa, and 31 sigma levels are used in the vertical. WRF and MM5 were run for 24 hours beginning at 2100 JST July 12th 2004. Initial and boundary conditions for both models are derived from the NCEP Final Analysis Data. Details of the configurations of control simulation by WRF and MM5 are summarized in the Appendix.

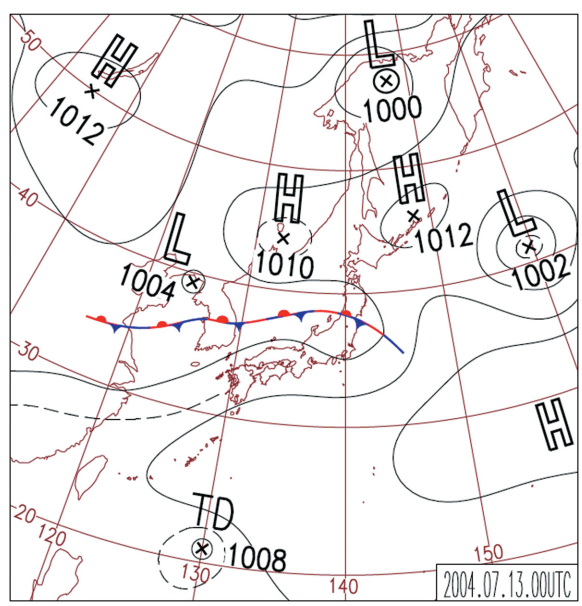

Fig. 1. Surface Weather Chart on 0900 Japan Standard Time (JST) July 13th 2004.

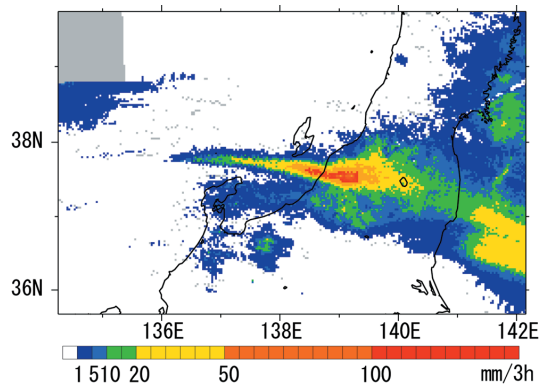

Fig. 2. Three-hourly accumulated precipitation at 0900 JST July 13th, 2004. Radar AMeDAS (Automated Meteorological Data Acquisition System) Data.

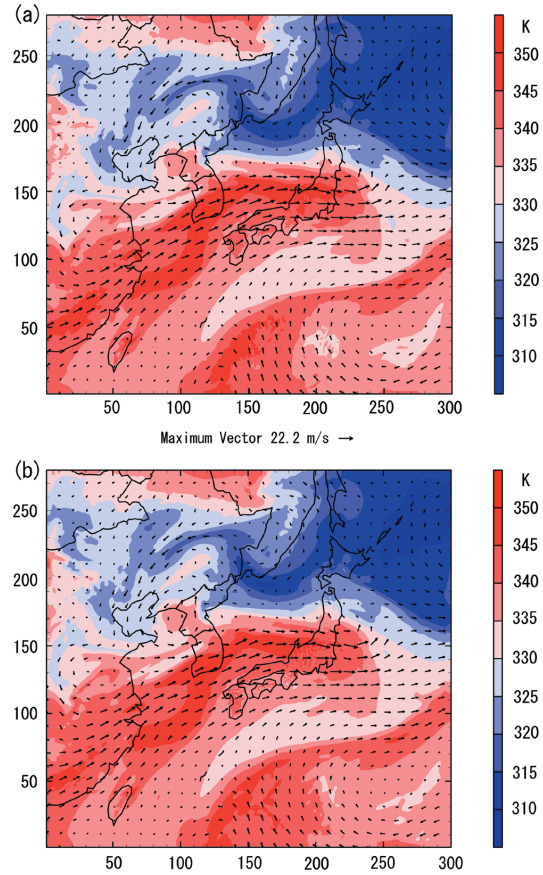

Fig. 3. Equivalent potential temperature and wind vector at 850 hPa level at 0900 JST July 13th from (a) WRF and (b) MM5. Axis is grid point of domain 1.

3. Results

Figure 3 shows the distribution of the equivalent potential temperature at 850 hPa from WRF and MM5. Both models produce similar results and simulate the front extended from the Sea of Japan to the Pacific Ocean.

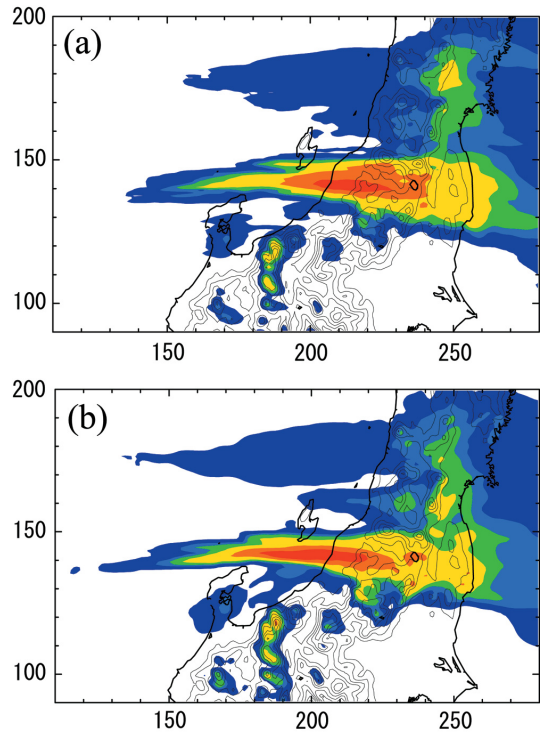

Fig. 4. Three-hourly accumulated precipitation at 0600 JST July 13th from (a) WRF and (b) MM5. Color scale is the same as that shown in Fig. 2. Axis is grid point of domain 2.

Figure 4 shows three-hourly accumulated precipitation from WRF and MM5. Both models simulate banded heavy rainfalls well and the precipitation patterns roughly agree with observations, although the phase is faster (Supplements 1, 2, and 3). In this study, we focus on the differences between WRF and MM5 in simulating the precipitation and vertical velocity fields. Thus, for the remainder of the paper we compare the simulated results from the two models at 0600 JST. The heaviest rainfall from WRF appears onshore, whereas it appears offshore for MM5. Figure 5 shows the distribution of the 850 hPa vertical velocity simulated by WRF and MM5. Positions of the strong upward wind correspond to the heavy rainfall areas, and the differences in the pattern between the two models are clearly confirmed. The strongest upward wind from WRF appears onshore, whereas it appears offshore for MM5. Another significant difference is that the vertical velocity from MM5 seems to be more smoothed than that from WRF.

Power spectral densities of 850hPa vertical velocity in the along-line (x) direction to the front were computed, referring to Takemi and Rotunno (2003). Data in the region of Fig. 5 and its east and west regions (from 32 to 288) are used. Figure 6 shows the differences between WRF and MM5. WRF maintains more energy for the wavelengths shorter than 60 km particularly 30 km when the fifth-order upwind scheme is set up in WRF. These results show that WRF simulates more detailed structure of the vertical velocity field than MM5.

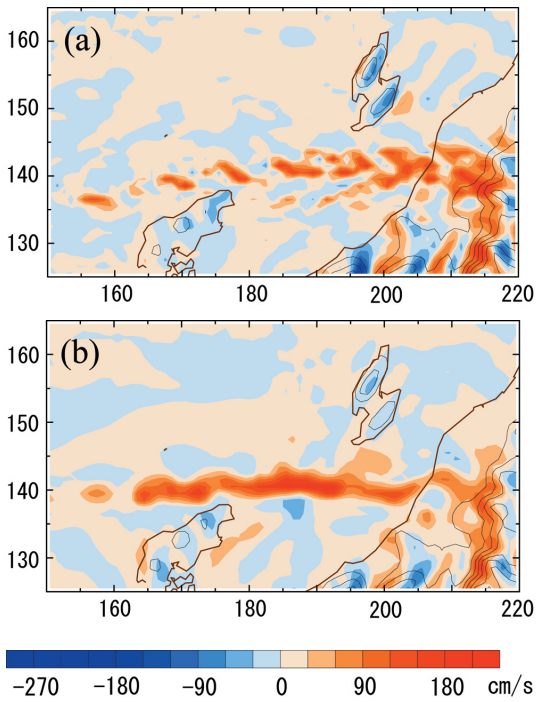

Fig. 5. Vertical velocity at 850hPa level at 0600 JST July 13th from (a) WRF and (b) MM5. Axis is grid point of domain 2.

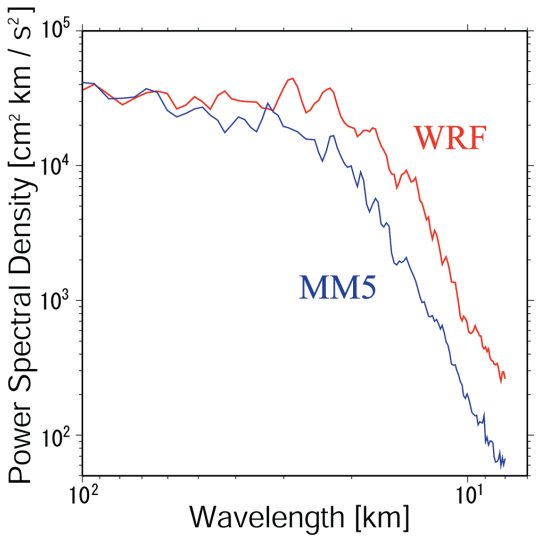

Fig. 6. Power spectral density of 850hPa vertical velocity at 0600 JST July 13th computed from WRF and MM5.

4. Discussion

The results from the simulations showed that the vertical wind velocity field from WRF has more detailed structure than that of MM5. Some may think that this is caused by the difference in the cloud microphysics used in WRF and MM5. We will show the results from additional numerical experiment where the other single moment bulk microphysics schemes are used in WRF. Figure 7 illustrates the fields of three-hourly accumulated precipitation and 850 hPa vertical velocity from the WRF using WSM6. Despite the fact that the difference in the model concept between Lin and WSM6 is larger than that between Lin and Goddard, precipitation pattern from the WRF using WSM6 is similar to that from the WRF using Lin (Figs. 4a and 7a). We can see that the strongest vertical velocity field from the WRF using WSM6 occurs onshore like the WRF using Lin. Comparing the vertical velocity field from WRF with WSM6 and MM5 shows the difference more clearly. Additionally, the vertical velocity field from WRF with WSM6 is less smoothed than that of MM5. These features are confirmed by changing to the other single moment bulk microphysics, Kessler warm rain model, WSM3 three-class simple ice model, and WSM5 five-class ice model (Fig. is omitted). This should be because the wind field is strongly affected by the large-scale convergence along the Baiu front, and thus the impact of the microphysics is relatively small in the present case.

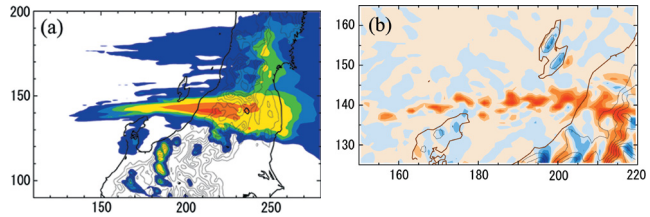

Fig. 7. Simulated results from the WRF using WSM6 micorophysics. Distribution of (a) three-hourly accumulated precipitation and (b) vertical velocity at 850 hPa at 0600 JST July 13th.

Another big difference besides the microphysics between WRF and MM5 modeling system is the numerical scheme for the model dynamics. In WRF, advection term uses fifth-order upwind scheme written in the Arakawa-C grid, which is equivalent to six-order centered scheme plus six-order diffusion term with a coefficient proportional to the Courant number (Skamarock et al. 2005). In contrast to this, MM5 uses second-order centered scheme and fourth-order diffusion scheme written in the Arakawa-B grid. Takemi and Rotunno (2003) investigated the effects of fourth-order diffusion on the development of linearly-organized moist convection and found that it has a significantly negative impact on the simulations. A series of numerical experiments by Kusaka et al. (2005) showed that the artificial second-order diffusion and explicit fourth-order numerical diffusion make the vertical velocity field smoothed, whereas the inherent, implicit sixth-order numerical diffusion in the fifth-order upwind scheme maintains detailed structure. Thus, it is reasonable that the higher-order differencing scheme without explicit numerical diffusion makes vertical velocity more detailed and power spectral density higher in WRF (e.g., Supplement 4). On the other hand, the difference in the position of the strongest vertical velocity between WRF and MM5 can be caused by the systematic error compared to observations of this MM5 simulation, although we can not definitely conclude this.

Recently, Kato and Aranami (2005) simulated the banded heavy rainfall, using the JMA-nonhydrostatic model (JMA-NHM) with three spatial resolutions, i.e., 1.5-, 5-, and 10-km horizontal grid spacing. Their results

show that the finest resolution model of the three, that is, the 1.5-km resolution model, succeeded in reproducing the banded heavy rainfall well. The other two coarser resolution models could not simulate the heavy rainfall well, but the finer resolution model of the two seemed to show the better outputs. The differences in the model configuration and initial and boundary conditions could be critical for the differences appearing in the present work and their results. It is a subject for future study to investigate the reason for the difference in the simulated results between WRF and NHM.

5. Conclusions

We conducted numerical simulations of heavy rainfall event along the Baiu front, using WRF and MM5 to investigate the differences between two models. Simulated results conclude as follows.

(1) The differences in the simulated precipitation pattern between WRF and MM5 are not large. However the position of the heaviest rainfall from WRF is found onshore which is almost same as that from the Radar AMeDAS. On the other hand, MM5 predicts the heaviest rainfall offshore.
(2) A difference in the position of the strongest vertical velocity is clearly found between WRF and MM5, which is consistent to the precipitation pattern.
(3) Additionally, the vertical velocity field of WRF is more detailed than that of MM5. Power spectral density of the vertical velocity shows clearly the difference.
(4) Sensitivity experiment indicates that the difference in the vertical velocity field between two models is due to the differences in the numerical scheme for the model dynamics, not in the cloud microphysics.

Comments and supplements

1. Three-hourly accumulated precipitation at 0600, 0900, 1200, 1500 JST on July 13th, 2004, which is estimated from the Radar AMeDAS Data. The color scale is the same as that shown in Fig. 2.
2. Three-hourly accumulated precipitation at 0300, 0600, 0900, 1200 JST on July 13th, 2004, which is estimated from the outputs of WRF. The color scale is the same as that shown in Fig 2.
3. Three-hourly accumulated precipitation at 0300, 0600, 0900, 1200 JST July 13th, 2004, which is estimated from the outputs of MM5. The color scale is the same as that shown in Fig 2.
4. Power spectral densities of the vertical velocity at 850 hPa level at 0600 JST. The green line is from the outputs of WRF with the 3rd-order scheme, while the red curve is from the calculation with the 5th-order one.

References

Dudhia, J., 1993: A nonhydrostatic version of the Penn State/NCAR Mesoscale Model: Validation tests and simulation of an Atlantic cyclone and cold front. *Mon. Wea. Rev.*, **121**, 1493–1513.

Durran, D. R., 1999: *Numerical methods for wave equations in geophysical fluid dynamics*, Springer-Verlag, 465 pp.

Kato, T., and K. Aranami, 2005: Formation factors of 2004 Niigata-Fukushima and Fukui heavy rainfalls and problems in the predictions using a cloud-resolving model. *SOLA*, **1**, 1–4.

Kusaka, H., A. Crook, J. Knievel, and J. Dudhia, 2005: Sensitivity of the WRF Model to advection and diffusion schemes for simulation of heavy rainfall along the Baiu front, *SOLA*, **1**, 177–180.

Skamarock, W. C., J. B. Klemp, J. Dudhia, D. O. Gill, D. M. Barker, W. Wang, and J. G. Powers, 2005: *A description of the advanced research WRF version 2*. NCAR/TN-468+STR, 88 pp.

Takemi, T., and R. Rotunno, 2003: The effects of subgrid model mixing and numerical filtering in simulations of mesoscale cloud systems. *Mon. Wea. Rev.*, **131**, 2085–2101.

Appendices

Table A1. Configuration of the WRF Model version 2.0.3.1 used in the present study.

Coordinate system	Mass coordinate system
Time integration	Time-split method using 3rd-order Runge-Kutta scheme with smaller time step for acoustic and gravity wave modes
Spatial discritization	5th-order upwind (horizontal) 3rd-order upwind (vertical)
Explicit numerical diffusion	Not used
Land surface	Noah-LSM
Surface layer	Monin-Obukhov similarity theory
Planetary boundary layer	MRF
Horizontal diffusion	2D-Smagorinsky
Short wave radiation	Dudhia
Long wave radiation	RRTM
Cloud microphysics	Lin
Cumulus parameterization	Kain-Fritch (domain 1)
Initial and boundary conditions	NCEP Final Analysis Data

Table A2. Configuration of the MM5 Model version 3.7.0 used in the present study.

Coordinate system	Sigma-P coordinate system
Time integration	Time-split method using 2nd-order Leap-Frog scheme with smaller time step for acoustic and gravity wave modes
Spatial discritization	2nd-order centered (horizontal) 2nd-order centered (vertical)
Explicit numerical diffusion	4th-order numerical diffusion
Land surface	Noah-LSM
Surface layer	Monin-Obukhov similarity theory
Planetary boundary layer	MRF
Horizontal diffusion	Artificial (numerical) diffusion
Short wave radiation	RRTM
Long wave radiation	RRTM
Cloud microphysics	Goddard (based on Lin)
Cumulus parameterization	Kain-Fritch (domain 1)
Initial and boundary conditions	NCEP Final Analysis Data

Manuscript received 29 August 2005, accepted 12 October 2005
SOLA: http://www.jstage.jst.go.jp/browse/sola/